InGaAs/GaAs/alkanethiolate radial superlattices

Ch. Deneke,[a] U. Zschieschang, H. Klauk, and O. G. Schmidt
Max-Planck-Institut für Festkörperforschung, Heisenbergstr. 1, D-70569 Stuttgart, Germany

(Received 4 September 2006; accepted 19 October 2006; published online 27 December 2006)

A radial InGaAs/GaAs/1-hexadecanethiol superlattice is fabricated by the roll-up of a strained InGaAs/GaAs bilayer passivated with a molecular self-assembled monolayer. The technique allows the formation of multiperiod inorganic/organic hybrid heterostructures. The authors investigate the radial superlattices in a detailed transmission electron microscopy study. The structure consists of 11 tightly bonded semiconductor/organic layers with thicknesses and chemical compositions accurately controlled by epitaxial growth and self-assembly. Their chemical analysis reveals that neither any detectable oxygen contamination nor amorphization is present at the superlattice interfaces. © *2006 American Institute of Physics*. [DOI: 10.1063/1.2424541]

Rolled-up micro- and nanotubes[1,2] have been created from a wide variety of material combinations[3–6] and are promising candidates for waveguides,[7,8] ring resonators,[9,10] transport experiments,[11] and electronic[12] as well as nanofluidic applications.[13] Good control over size[14] and lateral position[13] of nanotubes has been exerted, raising legitimate hope for a future scalable and highly integrative nanotechnology. More recently, it has been shown that rolled-up tubes mimic the cylindrical geometry of a radial crystal[15] and—in the case of multiple rotations—represent a crystalline/noncrystalline radial superlattice (RSL).[16] The roll-up of semiconductor/Langmuir-Blodgett films has been proposed as a technique to create semiconductor/organic RSLs,[17] but the microscopic structure of such hybrid RSLs has not been revealed so far.

Here, we create semiconductor/organic superlattices by rolling up a strained semiconductor bilayer functionalized with a molecular self-assembled monolayer (SAM). The roll-up procedure enables us to compose alternating layers of single-crystalline inorganic semiconductor heterostructures (InGaAs/GaAs) and functional organic layers (thiolate SAM) in a radial geometry. Cross sections of such RSLs are carefully prepared by targeted focused ion beam (FIB) etching and polishing.[7] This refined technique enables us to study the structure and geometry of well-selected RSLs in unprecedented detail. High-resolution (HR) and analytical transmission electron microscopy (TEM) reveal tightly wound RSLs with high-quality interfaces and precisely controllable layer thicknesses and chemical compositions.

For our semiconductor/organic radial superlattices, a monolayer of 1-hexadecanethiol was self-assembled on the GaAs surface of an epitaxial InGaAs/GaAs bilayer, which in turn was grown on top of an AlAs sacrificial layer on a GaAs (001) substrate. The InGaAs/GaAs/SAM trilayer was then released from the substrate by selectively etching away the AlAs with HF. The HF gained access to the sacrificial buffer through openings in the sample surface created by fine scratches. Due to the inherent strain—caused by the lattice mismatch between the InGaAs and the GaAs layer—the released bilayer together with the SAM rolls up into a nanotube [Fig. 1(a)]. The tube can perform a high number of rotations on the surface,[3] if the strained layer is underetched for a sufficiently long time. From the obtained rolled-up nanostructures thin lamellas were prepared by FIB etching and investigated by (HR)TEM. During TEM, chemical analysis of the tube wall was carried out (FIB preparation and TEM were performed by FIE, Eindhoven and Zeiss, Oberkochen, respectively. For details Ref. 18).

Figure 1(b) displays a scanning electron microscopy (SEM) image of a typical rolled-up nanotube. The tube has an inner diameter of about 360 nm and rolled up over a distance of 16 μm. SEM clearly resolves nine outer windings, which appear closely attached to each other. A bright field cross-sectional TEM overview image of a similar nanotube with an inner diameter of 375 nm is shown in Fig. 1(c). The tube is embedded by outer and inner metal regions, which protected the tube during sample preparation (see Ref. 18). To ensure that some part of the sample is thin enough for HR- TEM, the specimen was thinned inhomogeneously until the lower part of the tube was completely removed by the FIB etching. Between the metal materials, 11 tightly rolled-up windings are clearly visible. The tube wall comprises alternating dark and bright regions. The dark regions are typically assigned to crystalline material, whereas the

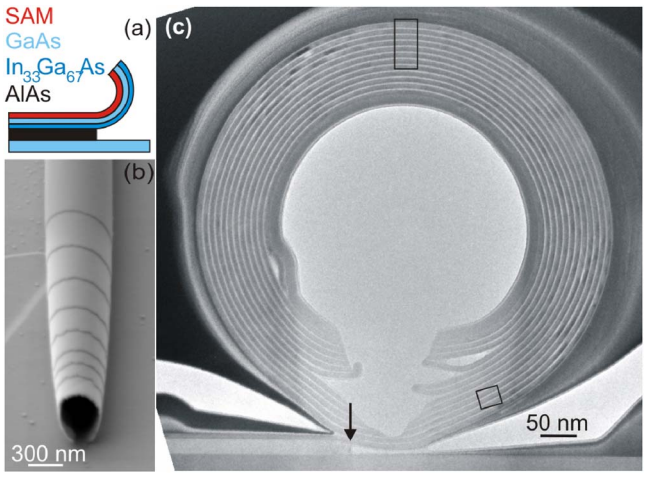

FIG. 1. (Color online) (a) Schematic illustration of the layer structure and the roll-up process. (b) Scanning electron microscopy image of a rolled-up radial superlattice with an inner diameter of 360 nm. (c) Bright field transmission electron microscopy image of a radial superlattice cross section. Black squares mark the areas of the TEM images presented in Figs. 2 and 3. The arrow points at the edge of the underetched sacrificial buffer layer.

[a]Electronic mail: c.deneke@fkf.mpg.de

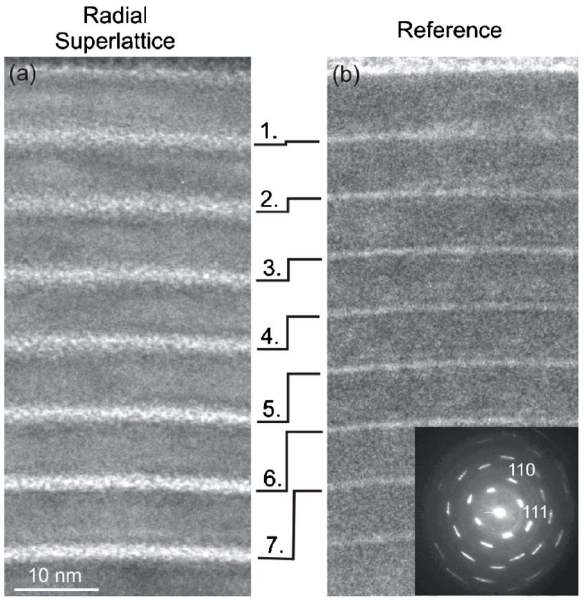

FIG. 2. (a) Magnified TEM image of the wall structure of the semiconductor/organic radial superlattice shown in Fig. 1. (b) TEM image of a reference structure fabricated from the semiconductor layer but without the SAM. The inset shows the diffraction pattern along the ⟨010⟩-zone axis. Elongated curved diffraction spots are visible due to the bent single crystal.

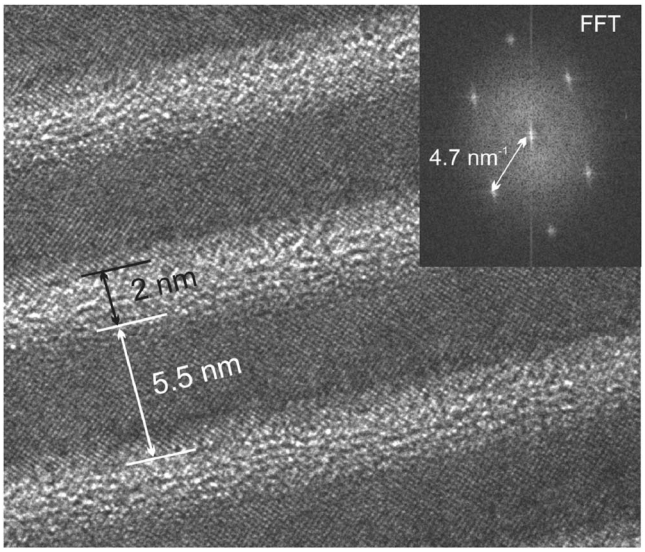

FIG. 3. High-resolution TEM image of the wall of the radial superlattice. The crystalline (noncrystalline) layer has a thickness of 5.5 nm (2 nm). The inset shows the Fourier transformation of the image.

bright region is usually assumed to consist of noncrystalline matter.[19] The radial superlattice is still attached to the substrate at the top of the back-etched buffer layer [see arrow in Fig. 1(c)]. This observation confirms that the position of the radial superlattice can be controlled by lithography and appropriate underetching times.[13]

The area marked by the upper rectangle in Fig. 1(c) is magnified by bright field TEM in Fig. 2(a). A reference structure without the SAM, but otherwise identical, is shown in Fig. 2(b). The dark crystalline layers in Fig. 2(a) are separated by about 2 nm thick bright noncrystalline regions. The TEM of the reference sample reveals dark crystalline layers of the same thickness, but the noncrystalline parts are much thinner (0.5 nm) than those in Fig. 2(a). The comparison of the two TEM images directly shows that seven periods of the semiconductor/organic radial superlattice are by one full period thicker than the InGaAs/GaAs reference sample without the SAM. Therefore, Fig. 2 indicates that the bright regions in Figs. 1(c) and 2(a) stem from the SAM, which is stable during the underetching process and forms—together with the semiconductor layer—an RSL.

The inset of Fig. 2(b) presents the diffraction pattern of a section of the rolled-up reference bilayer along the ⟨010⟩-zone axis. The fourfold symmetry of the zone axis is clearly observed, and the pattern is indexed for the reflection of a zinc blende lattice. The clear diffraction pattern indicates a high crystal quality of the sample. All reflections of the lattice planes are elongated into circle segments of diffraction rings, as we might expect for a curved crystal with nearly perfect cylindrical symmetry.[15]

Figure 3 shows a HR-TEM magnification of the area marked by the small rectangle in the lower part of Fig. 1. The TEM image confirms the existence of a crystal lattice in the dark regions of the tube wall. The bright regions show no clear lattice image as expected for the thiolate monolayer, because it lacks a perfect translation symmetry. The appearance of lattice fringes at some positions in the noncrystalline layer is attributed to information delocalization of the zinc blende lattice in the crystalline regions. The inferred thickness of the thiolate monolayer of about 2 nm is in excellent agreement with the length of the 1-hexadecanethiol molecule (2.1 nm, calculated using CS CHEM 3D PRO, version 7.0) and a chain tilt angle of 16° reported for methyl-therminated alkanethiolate monolayers on GaAs prepared from solution.[20] The measured 5.5 nm thickness of the rolled-up InGaAs/GaAs bilayer perfectly agrees with the thickness of the bilayer in the unrolled area of the same sample. This observation implies that practically no crystalline material is consumed during formation of the RSL interfaces, unlike to previous reports, where the semiconductor was not passivated by any organic layers.[15,16,21] The inset of Fig. 3 presents the two-dimensional fast fourier transformation (FFT) of the HR-TEM image, revealing the fourfold symmetry axis along the ⟨010⟩-zone axis, which we also identified in the diffraction pattern of the reference structure in Fig. 2(a). The FFT confirms that the zinc blende lattice of the epitaxial layer remains unaffected by the roll-up process.[15,16]

Since imaging tends to contaminate the samples with carbon, chemical analysis was performed on a second prepared cross section of a similar structure. The inset of Fig. 4 shows a high-angular dark field scanning TEM (STEM) image of the radial superlattice, and the white line marks the path of the stepwise chemical analysis (60 steps with 1 nm step width). Energy-dispersive x-ray (EDX) analysis was performed for Ga, In, As, and O. The carbon content was deduced from electron energy loss spectra (EELS) obtained at the same position. The measured normalized concentrations for the five elements are displayed as scatter plots in Fig. 4. The intensity modulation of the STEM image allows accurate correlation with the EDX and EELS scans through the radial superlattice.

From the sample growth and the measured layer thicknesses, we know the nominal structure and chemical composition of the superlattice. We plot the expected chemical concentrations of Ga, In, As, O, and C in the corresponding line scan panels of Fig. 4. The measured normalized concentrations of In, Ga, and As represent the semiconductor layers

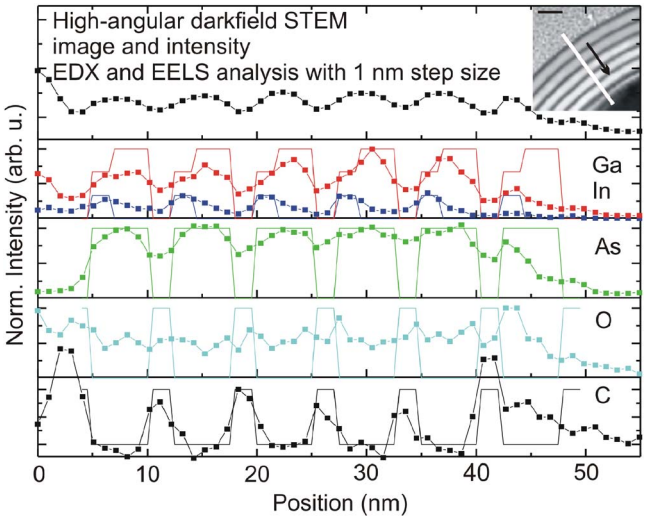

FIG. 4. (Color online) Chemical analysis across the wall of a radial superlattice. The inset shows a high-angular dark field STEM image of the investigated layers. The black curve is the intensity along the line marked in the inset. Chemical analysis (EDX and EELS) was performed along the white line for Ga, In, As, O, and C. In addition to the experimental data (dotted lines), the nominal expected intensities of the elements are indicated (solid lines).

within the radial superlattice. The maximum concentrations for these three elements are found in the bright regions of the dark field STEM image (corresponding to the dark regions in the bright field TEM image). The measured concentrations of In, Ga, and As follow the nominal profiles (within measurement accuracy) over five periods. The experimental values significantly diverge from the nominal ones only at the outer- and innermost regions of the radial superlattice, where the structure was affected by oxidation and delamination. The oxygen concentration across the tube wall remains nearly constant featuring no significant increase in the semiconductor nor in the organic layer. We explain the finite oxygen background level by a thin oxide layer that has formed on the top and bottom of the specimen during sample transportation from the FIB machine to the TEM. It is remarkable that the organic layers are practically free of any oxide. A tiny increase of oxygen is only faintly visible at some interface positions, where the SAM attaches to the next InGaAs/GaAs winding during the roll-up process. We are therefore confident that contaminations within the radial superlattice are hardly present and practically do not occur during the fabrication process of the RSLs. The normalized carbon concentration profile deduced from EELS shows modulations consistent with the intensity modulation of the STEM image. Carbon is only found at positions where the SAM is expected to be located. Together with the oxygen signal, we can safely say that the noncrystalline part is a pure hydrocarbon layer and does not consist of any amorphous oxide as reported previously for rolled-up nanotubes without the SAM.[16,21]

In conclusion, we have created multi-period semiconductor/organic radial superlattices by the roll-up of highly strained InGaAs/GaAs/alkanethiolate trilayers. Detailed cross-sectional TEM and chemical analysis shows that the radial superlattices consist of alternating crystalline semiconductor and organic layers with high-quality interfaces that are practically free of any contaminations. Since a strained crystalline layer can be combined deliberately with arbitrary combinations of organic or inorganic materials, our radial superlattices define a class of hybrid short-period heterostructures, which can be integrated on a single chip by standard lithographic techniques.

The authors acknowledge FEI Company for preparing the TEM lamella and performing the TEM of the radial superlattice (P. Persson). Carl Zeiss Company is acknowledged for one SEM image as well as the preparation and characterization of the reference sample (A. Orchowski). This work was financially supported by the BMBF (03N8711) and EC NoE Sandie.

[1] V. Ya. Prinz, V. A. Seleznev, A. K. Gutakovsky, A. V. Chekhovskiy, V. V. Preobrazhenskii, M. A. Putyato, and T. A. Gavrilova, Physica E (Amsterdam) **6**, 828 (2000).
[2] O. G. Schmidt and K. Eberl, Nature (London) **410**, 168 (2001).
[3] O. G. Schmidt, N. Schmarje, Ch. Deneke, C. Müller, and N.-Y. Jin-Phillipp, Adv. Mater. (Weinheim, Ger.) **13**, 756 (2001).
[4] V. Luchnikov, O. Sydorenko, and M. Stamm, Adv. Mater. (Weinheim, Ger.) **17**, 1177 (2005).
[5] O. Schumacher, S. Mendach, H. Welsch, A. Schramm, Ch. Heyn, and W. Hansen, Appl. Phys. Lett. **86**, 143109 (2005).
[6] M. Huang, C. Boone, M. Roberts, D. E. Savage, M. G. Lagally, N. Shaji, H. Qin, R. Blick, J. A. Nairn, and F. Liu, Adv. Mater. (Weinheim, Ger.) **17**, 2860 (2005).
[7] Ch. Deneke and O. G. Schmidt, Appl. Phys. Lett. **89**, 123121 (2006).
[8] S. Mendach, R. Songmuang, S. Kiravittaya, A. Rastelli, M. Benyoucef, and O. G. Schmidt, Appl. Phys. Lett. **88**, 111120 (2006).
[9] T. Kipp, H. Welsch, Ch. Strelow, Ch. Heyn, and D. Heitmann, Phys. Rev. Lett. **96**, 077403 (2006).
[10] R. Songmuang, A. Rastelli, S. Mendach, and O. G. Schmidt arxiv: cond-mat/0611261.
[11] S. Mendach, S. Mendach, O. Schumacher, H. Welsch, Ch. Heyn, W. Hansen, and M. Holz, Appl. Phys. Lett. **88**, 212113 (2006).
[12] O. G. Schmidt, C. Deneke, S. Kiravittaya, R. Songmuang, H. Heidemeyer, Y. Nakamura, R. Zapf-Gottwick, C. Müller, and N. Y. Jin-Phillipp, IEEE J. Sel. Top. Quantum Electron. **8**, 1025 (2002).
[13] Ch. Deneke and O. G. Schmidt, Appl. Phys. Lett. **85**, 2914 (2004).
[14] C. Deneke, C. Müller, N. Y. Jin-Phillipp, and O. G. Schmidt, Semicond. Sci. Technol. **17**, 1278 (2002).
[15] B. Krause, C. Mocuta, T. H. Metzger, Ch. Deneke, and O. G. Schmidt, Phys. Rev. Lett. **96**, 165502 (2006).
[16] Ch. Deneke, N.-Y. Jin-Phillipp, I. Loa, and O. G. Schmidt, Appl. Phys. Lett. **84**, 4475 (2004).
[17] V. Ya. Prinz, V. A. Seleznev, L. L. Sveshnikova, and J. A. Badmaeva, Proceedings of the Eighth International Symposium Nanostructures: Physics and Technology, St. Petersburg, Russia, 19–23 June 2000 (unpublished).
[18] Ch. Deneke, U. Zschieschana, H. Klauk, and O. G. Schmidt, arxiv: cond-mat/0612373.
[19] S. Amelinckx, D. van Dyck, J. van Landuyt, und G. van Tendeloo, *Handbook of Microscopy* (VCH, Weinheim, 1997), Vols. 1 and 2.
[20] C. L. McGuiness, A. Shaporenko, C. K. Mars, S. Uppili, M. Zharnikov, and D. L. Allara, J. Am. Chem. Soc. **126**, 5231 (2006).
[21] N. Y. Jin-Phillipp, J. Thomas, M. Kelsch, Ch. Deneke, R. Songmuang, and O. G. Schmidt, Appl. Phys. Lett. **88**, 033113 (2006).